Breast cancer-associated gene 3 interacts with Rac1 and augments NF-κB signaling *in vitro*, but has no effect on RANKL-induced bone resorption *in vivo*

CHEN YAO[1,2], KUAN-PING YU[1], WILLIAM PHILBRICK[1], BEN-HUA SUN[1],
CHRISTINE SIMPSON[1], CHANGQING ZHANG[2] and KARL INSOGNA[1]

[1]Department of Internal Medicine, Yale University School of Medicine, New Haven, CT 06520, USA;
[2]Department of Orthopaedics, Shanghai Jiaotong University Affiliated Shanghai
No. 6 People's Hospital, Shanghai 200233, P.R. China

Abstract. Breast cancer-associated gene 3 (BCA3) is a recently identified adaptor protein whose functions are still being defined. BCA3 has been reported to be an important regulator of nuclear factor-κB (NF-κB) signaling. It has also been reported to interact with the small GTPase, Rac1. Consistent with that observation, in the present study, BCA3 was found to interact with nuclear Rac1 in 293 cells and influence NF-κB signaling. Additional experiments revealed that depending on cell type, BCA3 augmented, attenuated or had no effect on NF-κB signaling *in vitro*. Since canonical NF-κB signaling is a critical downstream target from activated receptor activator of nuclear factor κB (RANK) that is required for mature osteoclast formation and function, BCA3 was selectively overexpressed in osteoclasts *in vivo* using the cathepsin K promoter and the response to exogenous receptor activator of nuclear factor κB ligand (RANKL) administration was examined. Despite its ability to augment NF-κB signaling in other cells, transgenic animals injected with high-dose RANKL had the same hypercalcemic response as their wild-type littermates. Furthermore, the degree of bone loss induced by a 2-week infusion of low-dose RANKL was the same in both groups. Combined with earlier

Correspondence to: Dr Chen Yao, Department of Orthopaedics, Shanghai Jiaotong University Affiliated Shanghai No. 6 People's Hospital, Shanghai 200233, P.R. China
E-mail: goldeyeboy@sjtu.edu.cn

studies, the data from our study data indicate that BCA3 can affect NF-κB signaling and that BCA3 plays a cell-type dependent role in this process. The significance of the BCA3/NF-κB interaction *in vivo* in bone remains to be determined.

Introduction

Breast cancer-associated gene 3 (BCA3), also known as A kinase interacting protein 1 (Akip1) was first identified in mRNA screens of breast and prostate cancer cell lines (1). BCA3 was found through a yeast two-hybrid screen as a protein of unknown function that interacted with the N-terminal 30 residues of PKAc (2). BCA3 was later characterized as an important regulator of nuclear factor-κB (NF-κB) signaling by interacting with p65 and protein kinase A (PKA) (3-5). BCA3 is highly conserved among human, mouse and other species. Multiple phosphorylation sites and functional domains, such as a proline-rich domain (1), and SH2 and SH3 binding sites have been predicted based on its conserved amino-acid sequence (6), which suggests that BCA3 can interact with a wide variety of proteins. Consistent with that prediction, BCA3 has been reported to interact with several other proteins in addition to p65 and PKA (7-9). The interaction of BCA3 with TAp73 has been reported to enhance the sensitivity of cervical cancer cells to irradiation (7). BCA3 is a KyoT2 binding protein and may compete with really interesting new gene 1 (RING1) in regulating Notch signaling (8). Moreover, BCA3 can interact with the mitochondrial localized apoptosis inducing factor (AIF) and increase cardiomyocyte tolerance to oxidant and ischemic stress (10). Some interactions cause post-translational modifications of BCA3. Thus, interaction with secretory protein with RING finger domain (SPRING) leads to the ubiquitination of BCA3 (11). Similarly, BCA3 is neddylated by its interaction with NEDD8 and inhibits NF-κB signaling (9).

BCA3 was also identified as a Rac1-interacting protein in a yeast 2-hybrid screen using an osteoclast cDNA library as bait (12). Rac1 plays an important role in colony stimulating factor 1 (CSF1)-induced cytoskeleton remodeling in mature osteoclasts and the overexpression of BCA3 in these cells attenuates CSF1-induced cytoskeletal remodeling (13). Both BCA3 and Rac1 have been reported to play a role in NF-κB

signaling (3,14,15). Thus, in this study, we sought to determine whether their interaction also plays a role in NF-κB signaling *in vitro*. Since it is unclear and controversial as to whether BCA3 suppresses or promotes NF-κB signaling, we selectively overexpressed BCA3 in osteoclasts and examined the *in vivo* response of these animals to receptor activator of nuclear factor-κB ligand (RANKL), given that NF-κB is required for RANKL-induced osteoclastogenesis and bone resorption (16,17).

Materials and methods

Generation of BCA3 transgenic mice. To generate animals with the expression of BCA3 restricted to osteoclasts, the full-length cDNA for murine BCA3 was inserted into exon 1 of the cathepsin K (Ctsk) gene in a C57BL/6 mouse genomic bacterial artificial chromosome (BAC) clone, which was then used to create a transgenic animal model. The BAC clone (RP23-422N18) encompassing the entire Ctsk locus was purchased from the BACPAC Resources Center (https://bacpacresources.org). The cDNA for BCA3 was cloned by RT-PCR as previously reported (12). The relevant portions of the targeting vector used to introduce the BCA3 cDNA into the Ctsk locus are shown in Fig. 1A.

Standard cloning techniques were used to assemble the targeting vector that included 23 bp from the 5' end of Ctsk exon 1, the entire BCA3 coding sequence (including the endogenous stop codon), a neomycin selection cassette flanked by frt sites (18), and 13 base pairs from the 3' end of exon 1. To ensure the efficient translation of BCA3 cDNA, the 9 bp 5' of the BCA3 cDNA initiation codon were derived from the endogenous BCA3 Kozak sequence. Following assembly, the BCA3-NEO segment was then PCR-amplified with oligonucleotide primers representing 70 b of the Ctsk sequence immediately 5' and 3' of exon 1, respectively, to provide flanking homology for targeted homologous recombination into exon 1 of the Ctsk gene. This construct was integrated into the Ctsk gene within the BAC clone by homologous recombination using the Red recombination system of bacteriophage λ as previously described (18-20). Selected clones were sequenced across both Ctsk-insert junctions to confirm proper integration. The Neo cassette was excised by inducing FLP recombinase F70L in the DH10B bacterial host of the recombined BAC clone (21).

The engineered Ctsk/BCA3 BAC clone was then microinjected into C57BL/6 X SJL F2 oocytes and transgenic animals were generated using standard techniques. Briefly, to generate zygotes for microinjection, 3-week old B6;SJLF1 females (JAX) were superovulated by IP injection with 5IU pregnant mare's serum gonadotropin and 46 h later, IP injection of 5IU human chorionic gonadotropin. Subsequent to the administration of human chorionic gonadotropin, the females were mated with B6;SJL F1 stud males (JAX) between the age of 10 weeks to 12 months. Females with a copulatory plug the following morning (0.5 dpc) were euthanized and zygotes were collected from oviducts. The engineered Ctsk/BCA3 BAC clone was microinjected at a concentration of 5 ng/μl in TE into the pronucleus of approximately 225 zygotes, and injected zygotes were transferred to the oviducts of pseudopregnant females after injection, 25-30/mouse, via standard embryo transfer surgery. At weaning, tail biopsies of pups resulting from microinjection were collected and genotyped, and 2 founder mice containing the transgene were identified. These founders were bred with 6-8 weeks old wild-type C57Bl/6 mice to establish 2 independent lines. This ensured that the transgenic animals remained heterozygous during breeding. Resultant transgenic mice were identified by PCR amplification of a unique Ctsk-BCA3 junction sequence. Transgenic animals and their wild type littermates, used in all experiments were studied at 12 weeks of age. For the bone density experiments, 10 transgenic animals (4 female, 6 male) and 16 wild type littermate controls (6 female, 10 male) were examined. For the RANKL infusion experiments, 10 transgenic animals (5 female, 5 male) and 9 wild type litter mate controls (5 female, 4 male) were examined. The use of animals in this study was approved by the Yale Animal Care and Use Committee.

Cells. The pZen murine fibroblast cell line (22) was a generous gift from Dr Lawrence Rohrschneider. The MC3T3E1 (preosteoblasts), 293, NIH3T3 (fibroblasts) and HeLa (cervical cancer) cell lines were purchased from the American Type Culture Collection (ATCC, Manassas, VA, USA). The pZen and MC3T3E1 cells were grown in α-MEM (Sigma-Aldrich, St. Louis, MO, USA) supplemented with 10% fetal bovine serum (FBS) (Atlanta Biologicals, Lawrenceville, GA, USA) and 1% P/S (Gibco, Grand Island, NY, USA). The 293, HeLa and NIH3T3 cells were grown in Dulbecco's modified Eagle's medium (DMEM; high glucose) supplemented with 10% FBS, 1% P/S and 10 mM sodium pyruvate (all from Gibco).

RNA isolation and qPCR. Total bone RNA from BCA3 transgenic and wild-type animals was isolated from the tibiae and femurs of mice by rapidly isolating the long bones, removing soft tissue and immediately placing them in liquid nitrogen. The bones were pulverized to a powder in liquid nitrogen and RNA isolated using TRIzol® (Invitrogen, Carlsbad, CA, USA) following the manufacturer's recommended protocol. cDNA was synthesized using the iScript cDNA synthesis kit (Bio-Rad, Hercules, CA, USA). TaqMan probes and primer sets for mouse BCA3 (Mm00498591) and β-glucuronidase (GusB, Mm00446953) were purchased from Applied Biosystems (Foster City, CA, USA) and RT-PCR was performed using iQ Supermix (Bio-Rad). qPCR was performed using a BioRad MyiQ2 detection system. All qPCR reactions were performed in duplicate and cycling conditions were 95˚C for 20 sec and 60˚C for 1 min for 40 cycles. The relative expression level of each transcript was determined using the comparative CT method using GusB as an endogenous reference.

Cloning, DNA transfection and luciferase assay. The NF-κB luciferase construct was a generous gift from Sankar Ghosh (Chair of Microbiology and Immunology Albert Einstein College of Medicine). Rac1 and different BCA3 constructs were cloned by RT-PCR as previously described (12). We divided the full length BCA3 protein into 3 fragments: fragment 1, 2 and 3 which correspond to amino-acid 1-75, 76-125, and 126-221 of full length BCA3 protein, respectively. The Rac1 cDNA was subcloned into the pEGFPC1 vector (Clontech, Mountain View, CA, USA) to generate a Rac1-EGFP fusion protein. The cells were plated one day prior to transfection in 24-well plates at a density of 4-8x10⁴/well. Rac1, full-length BCA3 or truncated BCA3 constructs, or empty pcDNA4 vector were

co-transfected with the NF-κB luciferase construct using the Extreme Gene HP reagent (Roche, Indianapolis, IN, USA) at a ratio of 1:3. Twenty-four hours after transfection, the cells were stimulated with or without tumor necrosis factor-α (TNF-α) (10 ng/ml) in culture medium containing 1% FCS for a further 24 h before harvesting for luciferase assay. Luciferase assays were performed using the dual luciferase reporter assay system with pGL4.73 vector (both from Promega, Madison, WI, USA) as the internal control. Data are presented as the fold increase over cells transfected with empty pGL3 basic vector.

Staining and confocal microscopy. The 293 cells were plated on glass chamber slides (BD Falcon, Bedford, MA, USA) and transfected with pEGFP-Rac1 vector and His tagged BCA3 vector using the Extreme Gene HP reagent as described above. Cells were cultured for 48 h after transfection and fixed with 3.7% formaldehyde (Thermo Scientific, Rockford, IL, USA). Cells were then stained with Alexa 555 conjugated anti-His tag antibody (Upstate, Lake Placid, NY, USA) for BCA3. The slides were imaged using a Zeiss LSM 710 Duo confocal microscope (Carl Zeiss Microimaging, Thornwood, NY, USA).

Immunoprecipitation and immunoblots. Anti-Rac1 antibody (Cat no. 05-389; Millipore, Billerica, MA, USA) was cross-linked to protein A agarose beads (Calbiochem, Darmstadt, Germany) using dimethyl pimelimidate (Sigma-Aldrich) prior to immunoprecipitation. The 293 cells were transfected with full-length His-tagged BCA3 or truncated His-tagged BCA3 constructs as described above. The cells were cultured for 48 h after transfection and whole cell lysates prepared using HTNG lysis buffer (50 mM HEPES, 150 mM NaCl, 1% Triton X-100, 10% glycerol, 1.5 mM $MgCl_2$ and 1 mM EGTA). Equal amounts of whole cell lysates were incubated with protein A agarose coupled Rac1 antibody at 4˚C overnight. Beads were washed 3 times in HTNG lysis buffer and bound proteins eluted using 1X Laemmli sample buffer (Bio-Rad) with heating to 95˚C. Equal volumes of eluted protein, and amounts of whole cell lysates equivalent to the input into the immunoprecipitation experiments, were subjected to sodium dodecyl sulfate-polyacrylamide gel electrophoresis (SDS-PAGE) and transferred onto nitrocellulose paper (Trans-Blot Transfer Medium; Bio-Rad). After SDS-PAGE and trans-blotting, the nitrocellulose membrane was probed with an anti-His antibody (Cat no. 05-949; Millipore). The blots were developed using HRP conjugated secondary antibodies (Cat no. W4021; Promega) followed by enhanced chemiluminescence detection (ECL detection kit; Amersham Inc., Piscataway, NJ, USA).

RANKL injection and minipump infusion. Recombinant murine soluble RANKL was generously provided by Amgen, Inc. (Thousand Oaks, CA, USA). The *in vivo* hypercalcemia assay using high-dose RANKL injections was performed as previously described by Lacey *et al* (23). Briefly, transgenic or wild-type animals were administered 1.5 mg/kg of RANKL subcutaneously every 12 h for 7 doses at which point the serum calcium concentration was measured. To assess RANKL-induced bone loss, the cytokine was infused for 2 weeks using Alzet osmotic minipumps (Durect, Cupertino, CA, USA). RANKL at a constant dose of 0.4 mg/kg/day or phosphate-buffered saline (PBS) was administered for 14 days using minipumps that deliver 0.25 µl/h. The pumps were equilibrated in 0.9% NaCl overnight at 37˚C and then implanted into an interscapular subcutaneous pocket in either control or BCA3 transgenic mice using Isothesia® (Butler Animal Health Supply, Dublin, OH, USA) for anesthesia. After 14 days of infusion, the animals were sacrificed and serum collected to measure type I collagen carboxyterminal telopeptide (CTX). Bones were harvested for densitometric analysis by microCT.

Bone density measurements. *In vivo* bone density measurements were performed by dual-energy X-ray absorptiometry using a PIXImus densitometer (Lunar, Madison, WI) as previously described (24). Anesthetized mice (ketamine at 100 mg/kg body wt and xylazine at 10 mg/kg body wt given i.p.) were placed in the prone position and scans performed with a 1.270-mm-diameter collimator, 0.762-mm line spacing, 0.380-mm point resolution, and an acquisition time of 5 min. The spine window is a rectangle spanning a length of the spine from T1 to the beginning of the sacrum. The femur window encompasses the entire right femur of each mouse. The coefficient of variation for total body bone mineral density (BMD) is 1.5%. Microcomputed tomography was performed as previously described (25). Briefly, femurs were stripped of soft tissue and stored in 70% EtOH at 4˚C. Specimens were analyzed in 70% EtOH by cone beam microfocus X-ray computed tomography using a Scanco µCT-35 instrument (Scanco, Brutissellen, Switzerland). Images were acquired at 55 kVp, with an integration time of 500 msec and an isometric voxel size of 6 mm. Segmentation of bone from marrow and soft tissue was performed in conjunction with a constrained Gaussian filter (support = 1; 3X3X3 voxel window; σ=0.8) to reduce noise, applying density thresholds of 250 and 420 for the trabecular and cortical compartments of the femur, respectively. Volumetric regions for trabecular analysis were selected within the endosteal borders of the distal femoral metaphysis to include the secondary spongiosa located 1 mm from the growth plate and extending 1 mm proximally. Cortical morphometry was quantified and averaged volumetrically through 233 serial cross-sections (1.4 mm) centered on the diaphyseal midpoint between proximal and distal growth plates. Both 2- and 3-D µCT data included bone volume to total volume fraction (BV/TV), and trabecular number (Tb.N), thickness (Tb.Th), spacing (Tb.Sp) and connectivity density (Conn.D). Cortical thickness, averaged for both cortices (Ct.Th), was also quantified.

Biochemical measurements. Serum type I collagen carboxyterminal telopeptide (CTX) was measured by EIA (Ratlaps EIA kit; Immunodiagnostic Systems Inc., Scottsdale, AZ, USA). Serum calcium was measured in the Yale New Haven Hospital Consolidated Laboratory (Department of Laboratory Medicine) using a multichannel autoanalyzer (Roche DPP Autoanalyzer).

Statistical analysis. An unpaired t-test or one-way ANOVA with Bonferroni post-hoc testing was used as indicated in the figure legends. Two-way ANOVA was used with Bonferroni post-hoc test to assess the change of CTX and bone mass data by µCT in the low-dose RANKL infusion experiment. Two-way ANOVA was also applied to the analysis of the effect of BCA3 on NF-κB signaling in different cell types (Fig. 6). Data presented are the means ± SEM. The error bars in figures
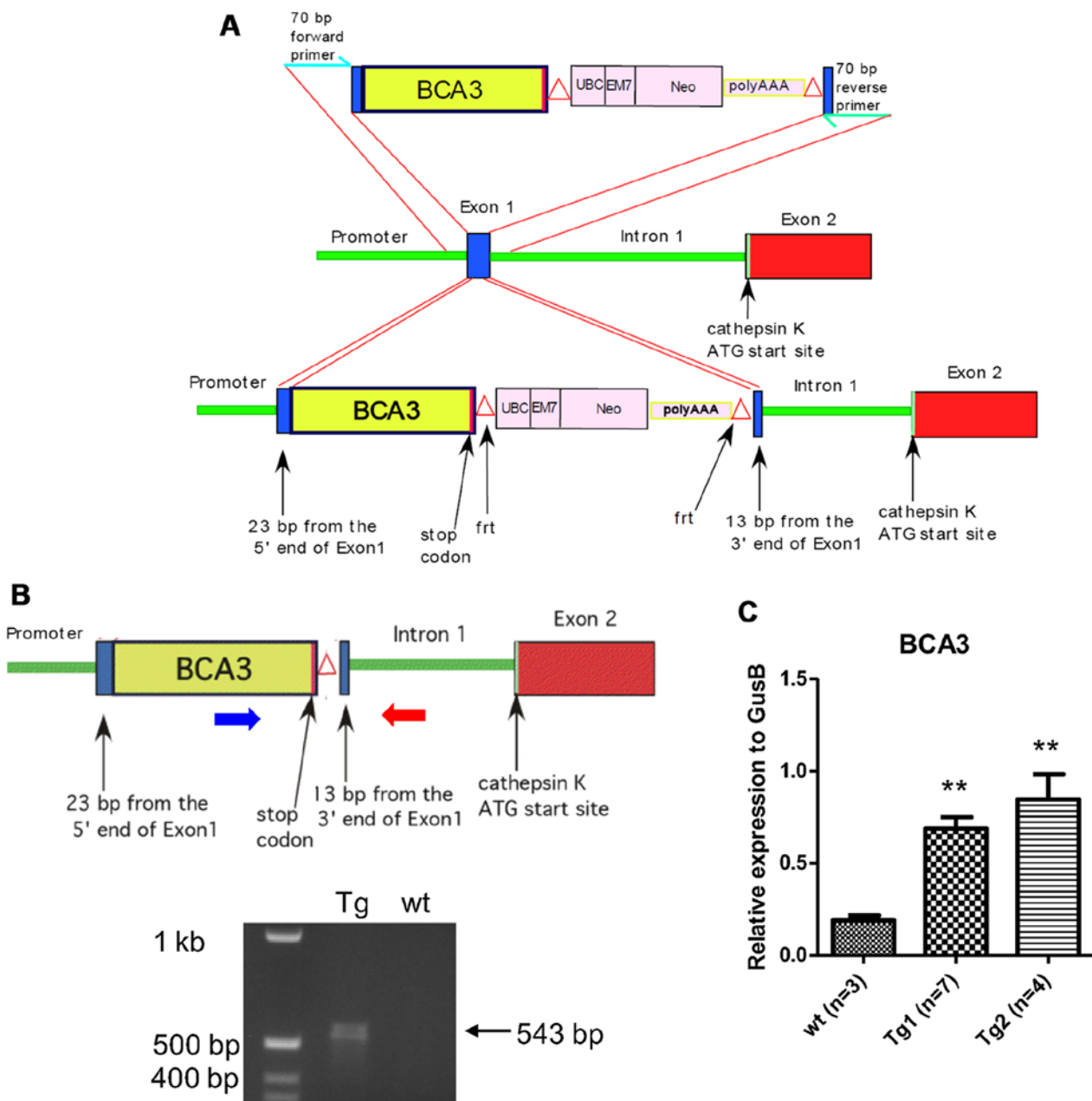
Figure 1. Development of breast cancer associated gene 3 (BCA3) transgenic mice with targeted overexpression of murine BCA3 in mature osteoclasts. (A) The targeting vector included 23 bp from the 5' end of cathepsin K (Ctsk) exon 1, the entire BCA3 cDNA sequence (including the endogenous stop codon), a neomycin selection cassette flanked by frt sites and 13 base pairs from the 3' end of exon 2. This construct was integrated into the Ctsk gene exon 1 within the BAC clone by homologous recombination. (B) Upper panel: after selecting positive clones, the Neo cassette was excised by inducing FLP recombinase F70L in the DH10B bacterial host of the recombined BAC clone. The blue and red large horizontal arrows show the location of the genotyping primers; Lower panel: agarose gel of PCR amplicons demonstrating the expected 543 bp fragment from the transgene. (C) The tibiae and femurs were isolated from mice from two different transgenic lines and RNA extracted. Real-time PCR demonstrated that both lines overexpress BCA3. Data were analyzed by unpaired t-test. (**p<0.01).

reflect SEM. A value of p<0.05 was considered to indicate a statistically significant difference.

Results

BCA3-Rac1 interaction promotes NF-κB signaling in 293 cells. BCA3 is thought to affect NF-κB signaling by shuttling PKA to the nucleus and enhancing the phosphorylation of p65 (4,5). Rac1 has also been reported to activate the NF-κB pathway although the details of that molecular mechanism remain unclear (26,27). Since, as noted, BCA3 can bind Rac1,

experiments were performed to determine the impact of this interaction on NF-κB signaling. The overexpression of BCA3 alone in 293 cells activated NF-κB signaling (Fig. 2A, left panel). The expression of BCA3 also robustly enhanced TNF-α-induced NF-κB signaling compared to the empty vector (EV) control (Fig. 2A, right panel). These data are consistent with those of published studies demonstrating that BCA3 augments NF-κB signaling in 293 cells (2-4). We have previously defined the region of BCA3 responsible for interacting with Rac1 by using three deletion constructs: fragment 1 (aa 1-75), fragment 2 (aa 76-125) and fragment 3 (aa 126-221) (12). Fragment 2 was
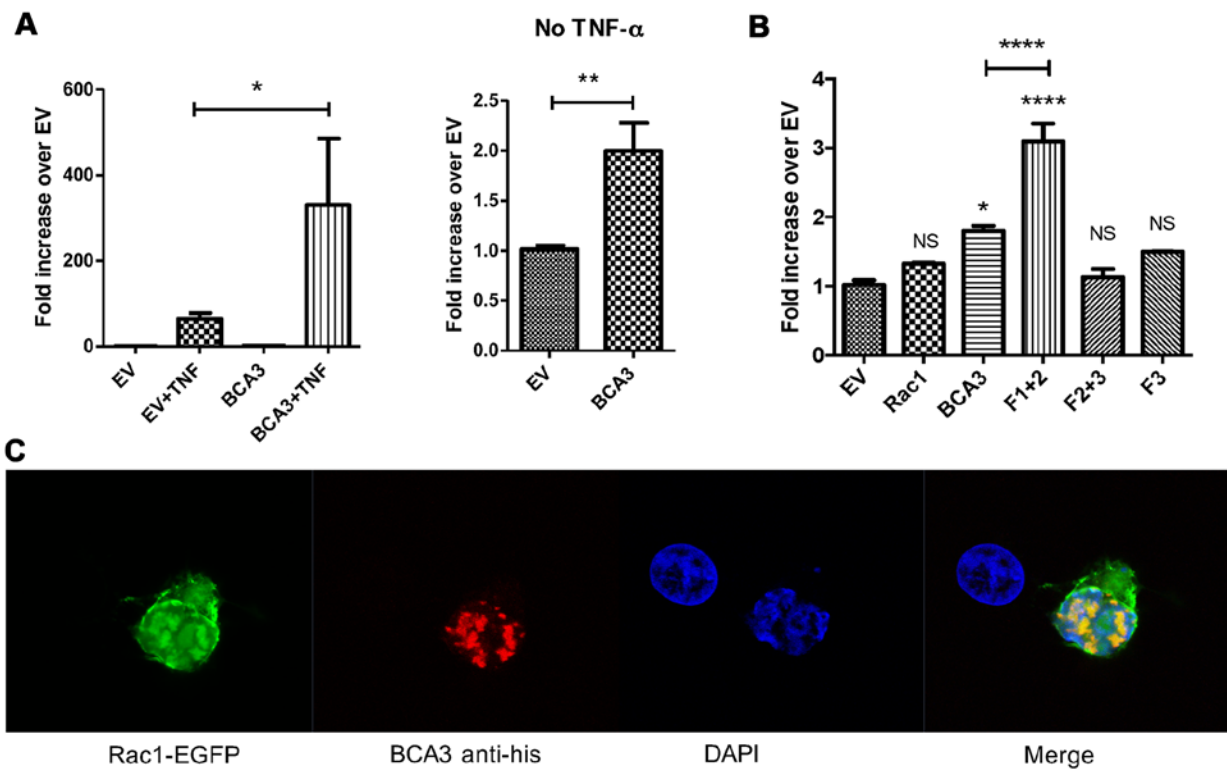
Figure 2. Breast cancer associated gene 3 (BCA3) augments nuclear factor-κB (NF-κB) signaling and co-localizes with Rac1 in 293 cells. (A) An NF-κB luciferase reporter construct and a BCA3 expression vector were co-transfected into 293 cells. Luciferase assays demonstrated that BCA3 significantly increased NF-κB activity after tumor necrosis factor-α (TNF-α) treatment (left panel; 10 ng/ml for 24 h). The right panel shows the effect of BCA3 overexpression on NF-κB signaling in the absence of TNF-α and is simply the data from columns 1 and 3 in the left panel presented on a different scale so the effect can be seen. Data were analyzed by an unpaired t-test. (B) Rac1, full length BCA3 or the indicated truncated BCA3 constructs were co-transfected with the NF-κB luciferase reporter into 293 cells. BCA3 fragment 1+2 augmented NF-κB signaling to a significantly greater extent than did either full-length BCA3 or fragment 2+3. Data were analyzed by one-way ANOVA with Bonferroni post-test corrections. (C) Vectors containing Rac1-EGFP and His-tagged, full-length BCA3 were co-transfected into 293 cells, stained and imaged by confocal microscopy. BCA3 and Rac1 co-localized primarily in the nucleus of 293 cells ($^*p<0.05$; $^{**}p<0.01$; $^{***}p<0.001$; NS, $p>0.05$). NS, not significant.

identified as a putative Rac1 binding site. In the present study, the overexpression of BCA3 fragment 1+2 alone activated NF-κB signaling, while fragment 2+3 or fragment 3 alone showed no activity (Fig. 2B). As previously reported, we were unable to individually express fragment 1 or 2 (12). The augmentation of NF-κB signaling by fragment 1+2 was even stronger than the wild-type full length BCA3. These results suggest that the amino terminal 125 amino acids of BCA3 contain an NF-κB activating sequence, while fragment 3 may have the function to prevent BCA3 being over-activated. The overexpression of Rac1 did not have a significant effect on NF-κB activity (Fig. 2B).

To investigate BCA3 Rac1 interactions in 293 cells, the cells were transfected with EGFP-tagged Rac1 and His-tagged BCA3. Confocal microscopy showed BCA3 staining to be primarily nuclear in a speckled pattern, while Rac1 was found both in the cytoplasm and nucleus (Fig. 2C). BCA3 and Rac1 fluorescence exhibited significant nuclear co-localization consistent with a molecular interaction (Fig. 2C). To further confirm a BCA3-Rac1 interaction, His-tagged BCA3 or His-tagged BCA3 fragments were transiently transfected into 293 cells, and lysates were prepared and immunoprecipitated with an antibody to Rac1. The Rac immunoprecipitates were examined by immunoblotting with an anti-His antibody. As shown in Fig. 3A, Rac1 co-precipitated full-length BCA3, fragment 1+2 and 2+3. By contrast, very little of

fragment 3 co-precipitated with Rac1 (Fig. 3A). As noted, fragments 1 and 2 could not be individually expressed (lanes 5 and 6).

When adjusted for the level of input (Fig. 3A, bottom panel), fragment 1+2 appeared to have Rac1 binding ability similar to full-length BCA3 and to have more activity than fragment 2+3. Since fragment 1+2 was also more effective at activating NF-κB than fragment 2+3, this raised the possibility that the interaction with Rac1 may augment the effect of BCA3 on NF-κB signaling. To examine this hypothesis, BCA3 and its fragments were co-transfected with Rac1 into 293 cells with the NF-κB reporter construct and luciferase assays performed (Fig. 3B). As these experiments required 3 simultaneous transfections, lesser amounts of DNA were used for each construct. When only 2 vectors were being analyzed (e.g., NF-κB reporter and full-length BCA3) an empty vector was also transfected to ensure that equivalent amounts of DNA were used in every experimental condition so that variation in the amount of DNA introduced into the cell would not confound the results. For this reason, although full-length BCA3 and fragment 1+2 both increased NF-κB activity when introduced into the cells alone (Fig. 2A and B), in the experiments summarized in Fig. 3, these increases did not reach statistical significance.

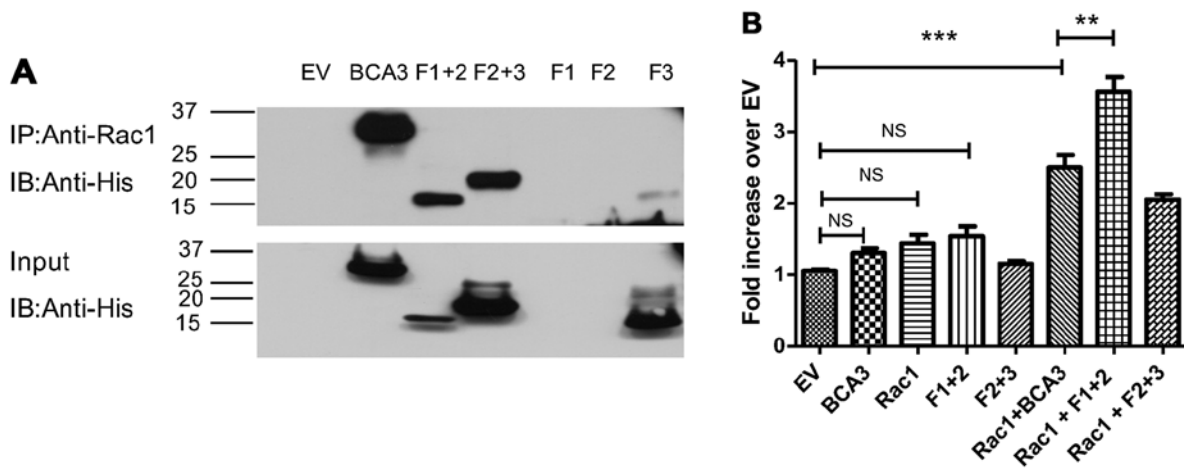As shown above, Rac1 alone did not stimulate NF-κB signaling (Fig. 3B). However, the expression of both Rac1 and

Figure 3. The breast cancer associated gene 3 (BCA3)-Rac1 interaction promotes nuclear factor-κB (NF-κB) signaling in 293 cells. (A) Upper panel: the indicated BCA3 constructs were transfected into 293 cells and immunoprecipitation performed using an anti-Rac1 antibody. Anti-His tag antibody was used to develop the blots. Full length BCA3, fragments 1+2 and 2+3 co-immunoprecipitated with Rac1 but there was almost no interaction of Rac1 with fragment 3. As shown in lanes 5 and 6, fragments 1 and 2 could not be individually expressed. Lower panel: inputs of the BCA3 constructs. (B) The indicated BCA3 constructs were co-transfected into 293 cells along with the Rac1 and the NF-κB luciferase reporter construct, and luciferase assays performed in the absence of tumor necrosis factor-α (TNF-α). Full-length BCA3 plus Rac1 and fragment 1+2 plus Rac1 significantly enhanced NF-κB activity. Data were analyzed by one-way ANOVA with Bonferroni post-test corrections (**p<0.01; ***p<0.001; NS, p>0.05). NS, not significant.

full-length BCA3 led to the synergistic activation of NF-κB. The expression of both Rac1 and fragment 1+2 was even more effective at activating NF-κB signaling, while Rac1 plus fragment 2+3 was less effective than Rac1 plus either full-length BCA3 or fragment 1+2.

Osteoclast-specific overexpression of BCA3 in mice. The role and importance of BCA3 as well as that of the Rac1/BCA3 interaction in regulating NF-κB signaling remain to be fully defined. Our previous study suggested that BCA3 may have an important function in osteoclasts (12). BCA3 has been reported to play an important role in NF-κB signaling, which is required for RANKL-dependent osteoclast formation and activation (28). We were unable to find a cell model of osteoclasts in which to test the interaction of BCA3 and NF-κB *in vitro*. Despite studies to the contrary (29), we have not been able to demonstrate cytokine-responsive NF-κB signaling in RAW 264.7 cells, which are a commonly used model of preosteoclasts. Primary murine preosteoclasts are extremely resistant to transfection even using lentiviral infection. Although we have successfully introduced one construct into primary pre-osteoclast cultures (30), given the relatively low efficiency of even this method, the introduction of multiple constructs required to study NF-κB signaling as was done for the cells lines just described, is not feasible in preosteoclasts. Therefore in an effort to clarify the function of BCA3 in osteoclasts *in vivo*, studies were conducted in transgenic mice selectively overexpressing BCA3 in osteoclasts. Since RANKL is required for normal osteoclasts function and is the final common effector of bone resorption *in vivo*, we hypothesized that if NF-κB signaling was augmented by BCA3 in osteoclasts, the bone-resorbing effects of RANKL would be enhanced.

A full-length BCA3 cDNA was introduced into exon 1 of the Ctsk gene contained in a BAC DNA clone as described above and summarized in Fig. 1A and B. Two transgenic lines were created and the presence of the transgene was confirmed by PCR genotyping. To confirm the overexpression of BCA3

in bone, RNA was extracted from tibiae and femurs from two different transgenic lines and their wild-type siblings and analyzed by qPCR. There was a significant increase in BCA3 transcript expression in both transgenic lines (Fig. 1C). Since line 2 showed a higher level of BCA3 transcript expression this line was used in subsequent experiments. Since Ctsk expression is restricted to late preosteoclasts and mature osteoclasts in bone, the overexpression of BCA3 in the whole bone tissue indicates a very robust overexpression of BCA3 in osteoclasts since these cells make up only a small fraction of the cellular material in bone.

BCA3 transgenic mice have normal bone density and serum levels of CTX. Bone density was measured by DXA in 12-week old transgenic mice and littermate controls. There were no statistical differences in total body BMD (0.0539±0.0005 vs. 0.0535±0.0006 g/cm^2, Tg vs. Wt, n=10 and 16 in Tg and Wt groups, respectively, p=NS) ; femur BMD (0.0840±0.0013 vs. 0.0853±0.0020 g/cm^2, Tg vs. Wt, n=10 and 16 in Tg and Wt groups, respectively, p=NS) or spinal BMD (0.0612±0.0016 vs. 0.0594±0.0011 g/cm^2, Tg vs. Wt, n=10 and 16 in Tg and Wt groups, respectively, p=NS) (Fig. 4A). Micro CT analyses revealed no statistical differences in the trabecular bone density in either the femur or spine (data not shown). Consistent with these data, serum CTX values were similar in transgenic and control animals, suggesting no change in osteoclast resorptive activity (12.72±1.020 vs. 12.10±2.344 ng/ml, Tg vs. Wt, n=4 and 9 in Tg and Wt groups respectively, p=NS) (Fig. 4B).

Transgenic line 1 also showed normal bone density both by DXA and μCT analysis (data not shown) and was not further studied since, as noted, the expression level of BCA3 was lower than in transgenic line 2.

BCA3 overexpression does not alter the in vivo resorptive response to RANKL. Age and gender-matched BCA3 transgenic mice and their wild-type siblings were treated with
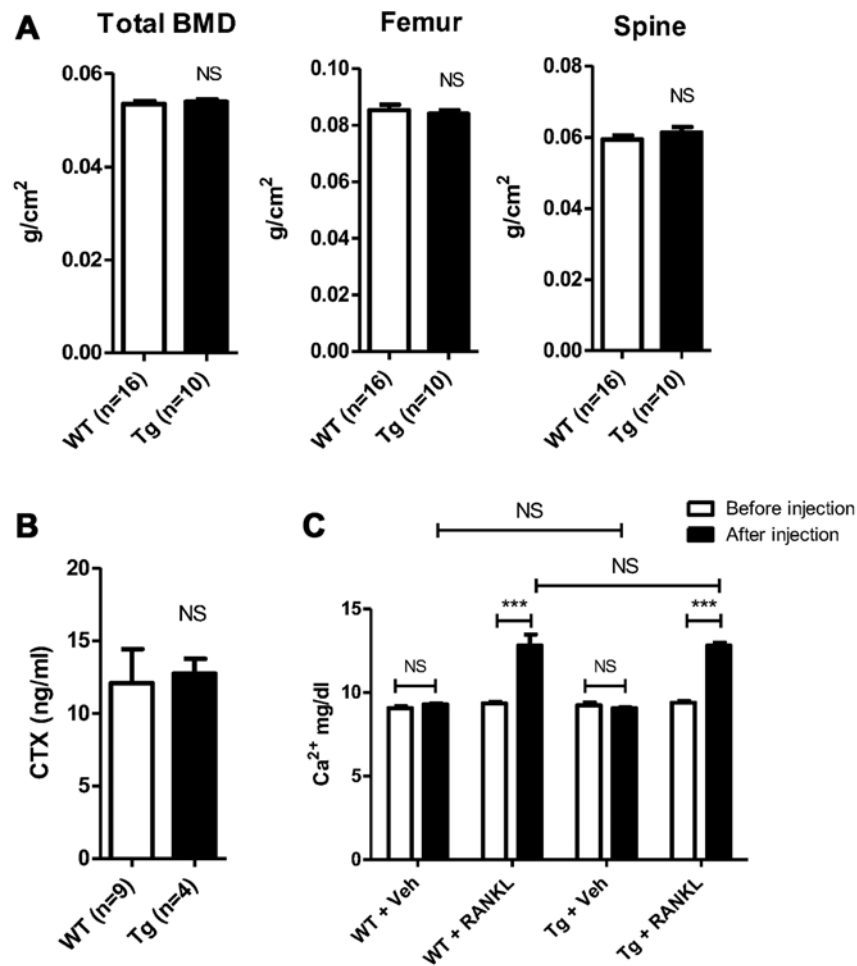
Figure 4. Equivalent baseline bone density and equivalent response to high-dose receptor activator of nuclear factor-κB ligand (RANKL) in Wt and breast cancer associated gene 3 (BCA3) transgenic mice. (A) Total and regional BMD by DXA in Wt and BCA3 transgenic mice. (B) Mean serum CTX values in Wt and BCA3 transgenic animals. (C) Calcemic response to short-term high-dose RANKL in Wt and BCA transgenic animals. Data were analyzed by an unpaired t-test ([***]p<0.001; NS, p>0.05). NS, not significant.

high-dose RANKL (1.5 mg/kg) or an equivalent volume of PBS administered subcutaneously every 12 h for a total of 7 doses. Serum calcium was measured before the first dose and after the final dose. There was no change in serum calcium levels with PBS treatment in either group (Tg, 9.2±0.2 vs. 9.1±0.1 mg/dl, baseline vs. PBS, n=3, p=NS; Wt, 9.1±0.1 vs. 9.3±0.1 mg/dl, baseline vs. PBS, n=3, p=NS) (Fig. 4C). As expected, RANKL treatment caused significant hypercalcemia in both groups compared to either baseline or to the vehicle treatment values in the animals receiving PBS (Tg, 9.4±0.1 vs. 12.8±0.2 mg/dl, baseline vs. RANKL, n=4, p<0.0001; Wt, 9.4±0.1 vs. 12.8±0.7 mg/dl, baseline vs. RANKL, n=4, p<0.0001) (Fig. 4C). However, there was no difference in the magnitude of hypercalcemia induced based on genotype. The serum calcium values following RANKL treatment did not differ between the 2 groups (12.8±0.2 vs. 12.8±0.7 mg/dl, Tg vs. Wt, n=4 in both groups, p=NS).

The low-dose infusion of RANKL leads to measurable bone loss in mice (31). Thus, to determine whether a lower dose and longer exposure to RANKL may reveal subtle differences in the osteoclastic response of wild-type and transgenic mice, both groups were administered RANKL (0.4 mg/kg/day) or PBS via an Alzet minipump for 14 days. After 14 days, the

mice were sacrificed and femurs and serum were obtained for μCT and CTX analyses.

RANKL caused significant and equivalent increases in serum CTX levels in both groups compared to PBS treatment (Tg, 17.3±3.2 vs. 60.8±9.0 ng/ml, n=4 vs. 6, PBS vs. RANKL respectively, p<0.05; Wt, 12.0±2.0 vs. 59.8±16.9 ng/ml, n=4 vs. 5, PBS vs. RANKL, respectively, p<0.05) (Fig. 5A). Although the fold increase in serum CTX levels was slightly greater in the Wt animals (3.5- vs. 5.0-fold, Tg vs. Wt), there was no difference in the mean serum CTX levels following RANKL infusion based on genotype (60.8±9.0 vs. 59.8±16.9 ng/ml, n=6 vs. 5, Tg vs. Wt, respectively, p=NS).

RANKL administration induced significant bone loss in both wild-type and transgenic mice compared to the PBS-infused animals. As shown in Fig. 5B (upper panel) 2 weeks of RANKL infusion resulted in a 53.6% decline in trabecular bone mass in the femur of transgenic animals and a comparable 50.5% decline in the controls. There was no difference in the mean trabecular bone volume following RANKL infusion based on genotype (3.82±1.22 vs. 3.36±1.6%, n=6 vs. n=5, Tg vs. Wt, respectively, p=NS). Trabecular number was slightly higher in the PBS-infused BCA transgenic animals than in the controls infused with saline (3.05±0.36 vs.
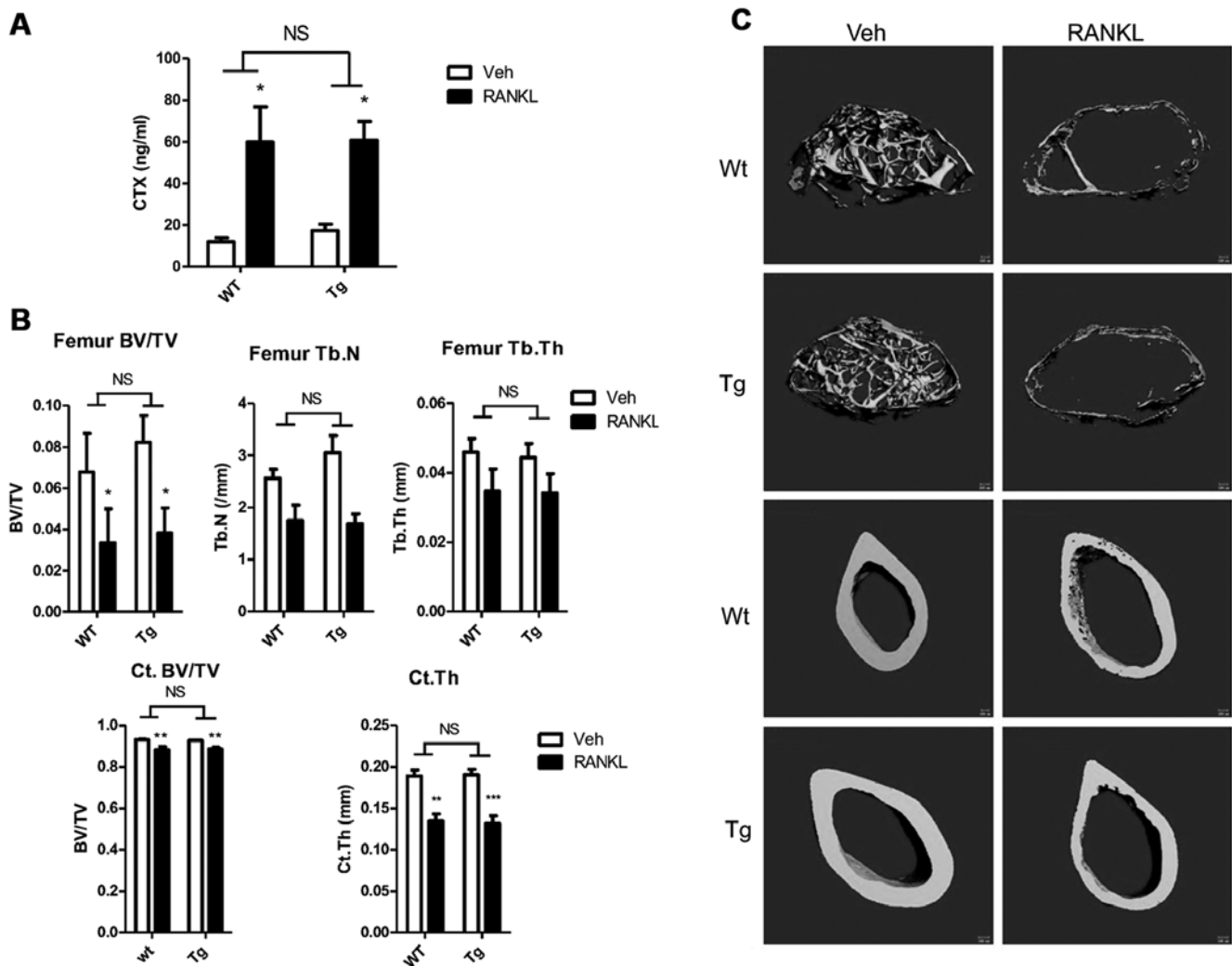
Figure 5. Response to long-term, low-dose receptor activator of nuclear factor-κB ligand (RANKL) infusion in Wt and breast cancer associated gene 3 (BCA3) transgenic animals. (A) RANKL treatment increased the mean CTX level compared to PBS treatment in both groups. No difference was observed between the 2 genotypes. (B) μCT analyses demonstrated that RANKL treatment significantly reduced bone mass in both trabecular and cortical envelopes. There was no difference between BCA3 transgenic and wild-type animals in the response to RANKL infusion. (C) Representative μCT images of femoral trabecular bone (upper four panels) or cortical bone (bottom four panels) from wild-type and transgenic animals treated either with vehicle (left column) or RANKL (right column) for two weeks. Data were analyzed by two-way ANOVA with Bonferroni post-test corrections. *p<0.05, **p<0.01 and ***p<0.001 refer to differences between the vehicle-infused and RANKL-infused animals of each genotype. NS, not significant, i.e., p>0.05.

2.56±0.17/mm, n=3 vs. 4; Tg vs. Wt, p=NS); however trabecular number was similar in both groups following RANKL administration (1.69±0.19 vs. 1.75±0.30/mm, Tg vs. Wt, p=NS). The percentage decrease in trabecular thickness in the RANKL-infused compared to the PBS-infused animals (23.1 vs. 24.4%, Tg vs. Wt) and the final values for the parameter (0.034±0.006 vs. 0.035±0.006 mm, n=6 vs. 5, Tg vs. Wt, respectively, p=NS) did not differ between the 2 groups. Cortical bone volume was similar in the 2 groups following saline infusion and declined by the same extent with RANKL treatment (4.5 vs. 5.0%, Tg vs. Wt) such that the values after RANKL infusion did not differ (88.61±0.92 vs. 88.30±1.31%, n=6 vs. 4, Tg vs. Wt, respectively, p=NS) (Fig. 5B, lower panel). Similarly, cortical thickness did not differ in either the saline-treated (0.190±0.007 vs. 0.189±0.007 mm, n=4 vs. 4, Tg vs. Wt, respectively, p=NS) or RANKL-treated (0.131±0.009 vs. 0.134±0.009 mm, n=6 vs. 4, Tg vs. Wt, respectively, p=NS) groups based on genotype.

As with all other parameters, RANKL induced a significant decline in this parameter that was equivalent in both groups of animals (Fig. 5B, lower panel). Fig. 5C shows representative images of cortical and trabecular bone from saline and RANKL-infused animals. In both RANKL-treated groups, marked loss of trabecular bone as well as cortical thinning are evident.

Effect of BCA3 on NF-κB signaling is cell-type dependent. Although BCA3 augments NF-κB signaling in 293 cells, it has also been reported to inhibit the NF-κB pathway in HeLa cells (9). Thus, to investigate the impact of BCA3 on NF-κB signaling in cells other than the 293 line, experiments were conducted in HeLa cells, pZen cells (a mouse embryonic fibroblast line overexpressing the CSF1 receptor), MC3T3E1 cells (a murine osteoblast-like cell line) and NIH3T3 cells. The pZen cells differ from NIH3T3 cells in that they are transformed and have tumorigenic potential (22). In pZen cells, BCA3
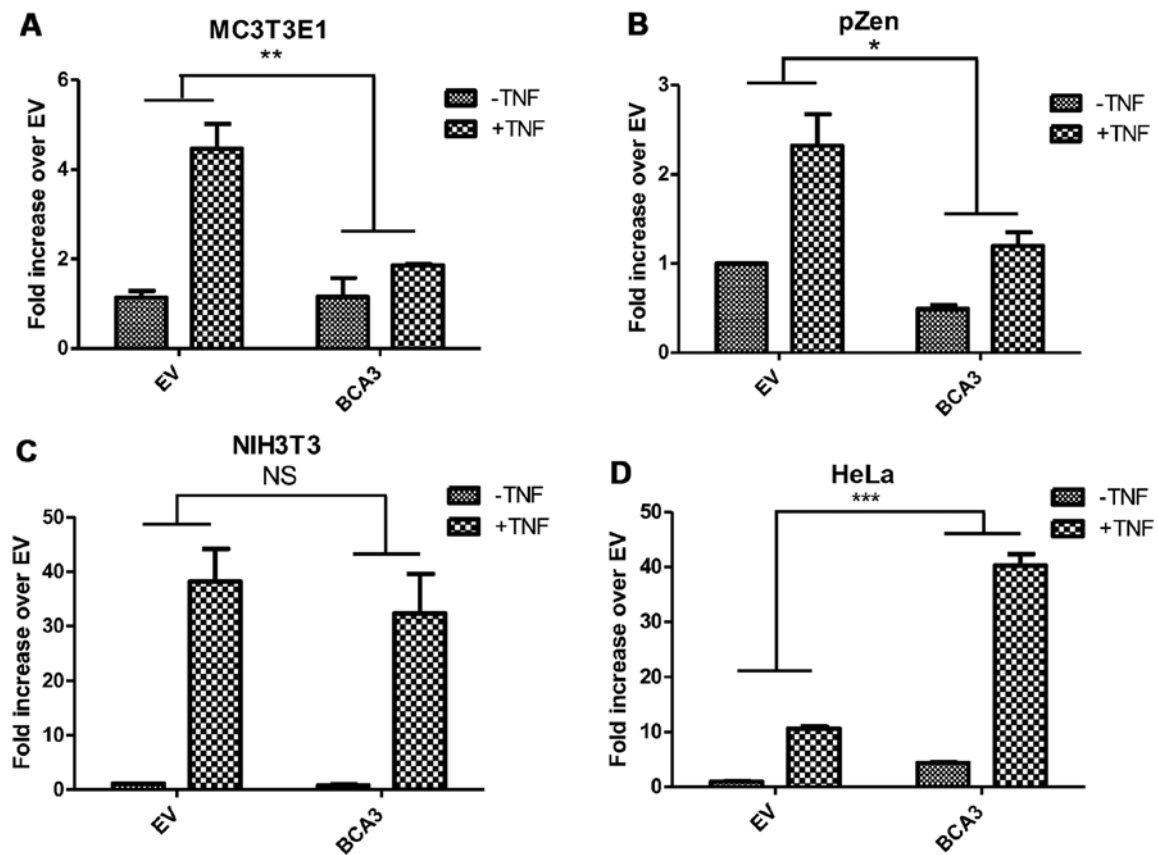
Figure 6. The effect of breast cancer associated gene 3 (BCA3) on nuclear factor-κB (NF-κB) signaling is cell-type dependent. Cells were transfected with full-length BCA3 and treated with or without 10 ng/ml tumor necrosis factor-α (TNF-α). (A and B) BCA3 attenuates NF-κB signaling before and after TNF-α treatment in MC3T3E1 and pZen cells. (C) BCA3 has no effect on NF-κB signaling in NIH3T3 cells. (D) BCA3 augments NF-κB signaling in HeLa cells. Data were analyzed by two-way ANOVA (*p<0.05; **p<0.01; NS, p>0.05). NS, not significant.

inhibited NF-κB signaling both in the absence and presence of TNF-α treatment (Fig. 6B). The results in MC3T3E1 cells were similar to those in pZen cells with an even greater inhibition of TNF-α-induced NF-κB signaling (Fig. 6A). However, BCA3 had no effect on NF-κB signaling in NIH3T3 cells (Fig. 6C). In contrast to the findings in these 2 cell lines, BCA3 significantly increased NF-κB signaling in HeLa cells (Fig. 6D).

Discussion

BCA3 was first characterized as a proline-rich protein over-expressed in breast and prostate cancer cells. Bioinformatics studies have identified multiple functional sites in its coding sequence, including a PDZ domain, a proline-rich domain, multiple SH2 domains and phosphorylation sites. Although the functions of BCA3 are largely unknown, its multiple predicted functional sites suggest that it may be an adaptor protein in signaling pathways. Consistent with this notion BCA3 has been reported to interact with several proteins including TAp73, Rac1, PKA, p65 and mitochondrial AIF.

The role of BCA3 in NF-κB signaling is an area of present interest. The BCA3-p65 interaction has been reported to facilitate the nuclear retention and phosphorylation of p65, thereby enhancing NF-κB signaling (3). Moreover the level of BCA3 expression modulates PKA-dependent p65 phosphorylation in HEK293 and MCF7 cells (4). The present study demonstrated that BCA3 robustly increased NF-κB activity when overex-

pressed in 293 cells and synergized with TNF-α in activating NF-κB-dependent transcription. In addition, c-terminally truncated BCA3 was a more potent agonist than the full-length protein, suggesting that the last 96 amino acids of BCA3 may have inhibitory activity. Consistent with our data that fragment 1+2 most effectively activates NF-κB signaling, p65 has been reported to interact with a region of BCA3 encoded by exon 4 (5), which is contained in fragment 2. However the carboxyterminal exons 5 and 6 of BCA3 reportedly interact with PKA (5). We found that fragment 1+2, which lacks exons 5 and 6, effectively activated NF-κB signaling while fragment 2+3, which contains exons 5 and 6 of BCA3 did not.

We have previously characterized BCA3 as a Rac1-interacting protein in osteoclasts. In the present study we extended this finding to 293 cells. In these cells the interaction occurred primarily in the nucleus, while in osteoclasts it was particularly prominent in the perinuclear region (12). In 293 cells, Rac1 and BCA3 synergized in promoting NF-κB activity. Rho family small GTPases such as Rac1 are able to activate NF-κB signaling although the mechanism is still unclear (26,32,33). Unlike Rac2 and Rac3, Rac1 has a strong polybasic region, which contains a nuclear localization signal (34-36). Geranylgeranyl modification of the carboxyterminus of Rac1, which binds to RhoGDI, results in cytoplasmic localization of Rac1. However, it has been shown that Rac1 accumulates in the nucleus during the G2 phase of the cell cycle and promotes cell division (34). In the present study, the

overexpression of wild-type Rac1 in 293 cells, had no effect on NF-κB signaling, since 293 cells express minimal amounts of BCA3 (10). The co-transfection of BCA3 with Rac1 greatly enhanced NF-κB activity and it is possible that BCA3 functioned as a molecular shuttle to bring Rac1 into the nucleus. How the Rac1/BCA3 interaction results in synergistic activation of NF-κB signaling is currently unclear.

This study also confirmed that fragment 2 of BCA3 was responsible for its interaction with Rac1 since co-immunoprecipitation experiments demonstrated that fragments 1+2 and 2+3, but not fragment 3 alone were pulled down with Rac1. Fragment 1+2 showed more robust interaction with Rac1 than did fragment 2+3 or full-length BCA3 suggesting an inhibitory effect of fragment 3. Consistent with this notion and with our hypothesis that fragment 2 contains the binding site for Rac1, it was fragment 1+2 that best synergized with Rac1 in activating NF-κB signaling.

NF-κB signaling is required for osteoclast differentiation, activation and survival (28,37,38). The RANK signaling cascade entrains the NF-κB complex and is critical to the resorptive effects of RANKL (28). RANKL potently activates NF-κB signaling in mature osteoclasts (28). Since BCA3 modulates NF-κB signaling, we hypothesized that it would impact the actions of RANKL by altering RANKL-dependent NF-κB signaling in preosteoclasts and mature osteoclasts. However, restricted overexpression of BCA3 in osteoclasts did not alter the skeletal phenotype of transgenic animals. To determine whether stressing the skeletons of these animals with exogenous RANKL would uncover a functionally significant change in RANKL activity, transgenic mice were tested for RANKL tolerance using two treatment strategies. We found that overexpression of BCA3 in osteoclasts did not alter the response to either short-term high-dose or longer-term lower dose RANKL administration. These data suggest that BCA3 is not a major regulator of NF-κB signaling in mature osteoclasts. Since BCA3 expression in our transgenic mice was restricted in its expression to mature osteoclasts and perhaps late preosteoclasts, our data do not preclude the possibility that BCA3 plays an important role in NF-κB-dependent signaling in early osteoclast differentiation.

The role of BCA3 in NF-κB signaling remains controversial. Although studies using 293 cells and breast cancer cell lines have indicated that BCA3 augments NF-κB signaling, it also has been reported to suppress NF-κB signaling in HeLa cells (9). By contrast, another group (3) reported that BCA3 enhanced the nuclear retention and phosphorylation of p65 in HeLa cells, consistent with enhanced of NF-κB signaling. In this study, the effects of BCA3 on NF-κB signaling were cell-type specific. We found that overexpression of BCA3 could augment, attenuate or have no effect on NF-κB signaling depending on the cellular context. These data suggest that the effect of BCA3 on NF-κB signaling may depend on its interacting partners, which may be cell type-specific. The significance of the BCA3/NF-κB interaction *in vivo* remains to be determined.

Acknowledgements

References

1. Kitching R, Li H, Wong MJ, Kanaganayakam S, Kahn H and Seth A: Characterization of a novel human breast cancer associated gene (BCA3) encoding an alternatively spliced proline-rich protein. Biochim Biophys Acta 1625: 116-121, 2003.
2. Sastri M, Barraclough DM, Carmichael PT and Taylor SS: A-kinase-interacting protein localizes protein kinase A in the nucleus. Proc Natl Acad Sci USA 102: 349-354, 2005.
3. Gao N, Asamitsu K, Hibi Y, Ueno T and Okamoto T: AKIP1 enhances NF-kappaB-dependent gene expression by promoting the nuclear retention and phosphorylation of p65. J Biol Chem 283: 7834-7843, 2008.
4. Gao N, Hibi Y, Cueno M, Asamitsu K and Okamoto T: A-kinase-interacting protein 1 (AKIP1) acts as a molecular determinant of PKA in NF-kappaB signaling. J Biol Chem 285: 28097-28104, 2010.
5. King CC, Sastri M, Chang P, Pennypacker J and Taylor SS: The rate of NF-κB nuclear translocation is regulated by PKA and A kinase interacting protein 1. PLoS One 6: e18713, 2011.
6. Leon DA and Cànaves JM: In silico study of breast cancer associated gene 3 using LION Target Engine and other tools. Biotechniques 35: 1222-1226, 1228, 1230-1231, 2003.
7. Leung TH and Ngan HY: Interaction of TAp73 and breast cancer-associated gene 3 enhances the sensitivity of cervical cancer cells in response to irradiation-induced apoptosis. Cancer Res 70: 6486-6496, 2010.
8. Qin HY and Han H: Effect of KyoT2 binding protein KBP1 on RBP-J-mediated transcriptional activity. Xi Bao Yu Fen Zi Mian Yi Xue Za Zhi 20: 544-547, 2004 (In Chinese).
9. Gao F, Cheng J, Shi T and Yeh ET: Neddylation of a breast cancer-associated protein recruits a class III histone deacetylase that represses NFkappaB-dependent transcription. Nat Cell Biol 8: 1171-1177, 2006.
10. Sastri M, Haushalter KJ, Panneerselvam M, Chang P, Fridolfsson H, Finley JC, Ng D, Schilling JM, Miyanohara A, Day ME, *et al*: A kinase interacting protein (AKIP1) is a key regulator of cardiac stress. Proc Natl Acad Sci USA 110: E387-E396, 2013.
11. Hashimoto M, Murata E and Aoki T: Secretory protein with RING finger domain (SPRING) specific to *Trypanosoma cruzi* is directed, as a ubiquitin ligase related protein, to the nucleus of host cells. Cell Microbiol 12: 19-30, 2010.
12. Yu KP, Itokawa T, Zhu ML, Syam S, Seth A and Insogna K: Breast cancer-associated gene 3 (BCA3) is a novel Rac1-interacting protein. J Bone Miner Res 22: 628-637, 2007.
13. Sakai H, Chen Y, Itokawa T, Yu KP, Zhu ML and Insogna K: Activated c-Fms recruits Vav and Rac during CSF-1-induced cytoskeletal remodeling and spreading in osteoclasts. Bone 39: 1290-1301, 2006.
14. Diebold I, Djordjevic T, Hess J and Görlach A: Rac-1 promotes pulmonary artery smooth muscle cell proliferation by upregulation of plasminogen activator inhibitor-1: role of NFkappaB-dependent hypoxia-inducible factor-1alpha transcription. Thromb Haemost 100: 1021-1028, 2008.
15. Williams LM, Lali F, Willetts K, Balague C, Godessart N, Brennan F, Feldmann M and Foxwell BM: Rac mediates TNF-induced cytokine production via modulation of NF-kappaB. Mol Immunol 45: 2446-2454, 2008.
16. Yu M, Qi X, Moreno JL, Farber DL and Keegan AD: NF-κB signaling participates in both RANKL- and IL-4-induced macrophage fusion: Receptor cross-talk leads to alterations in NF-κB pathways. J Immunol 187: 1797-1806, 2011.
17. Yamashita T, Yao Z, Li F, Zhang Q, Badell IR, Schwarz EM, Takeshita S, Wagner EF, Noda M, Matsuo K, *et al*: NF-kappaB p50 and p52 regulate receptor activator of NF-kappaB ligand (RANKL) and tumor necrosis factor-induced osteoclast precursor differentiation by activating c-Fos and NFATc1. J Biol Chem 282: 18245-18253, 2007.
18. Valenzuela DM, Murphy AJ, Frendewey D, Gale NW, Economides AN, Auerbach W, Poueymirou WT, Adams NC, Rojas J, Yasenchak J, *et al*: High-throughput engineering of the mouse genome coupled with high-resolution expression analysis. Nat Biotechnol 21: 652-659, 2003.

19. Copeland NG, Jenkins NA and Court DL: Recombineering: A powerful new tool for mouse functional genomics. Nat Rev Genet 2: 769-779, 2001.
20. Liu P, Jenkins NA and Copeland NG: A highly efficient recombineering-based method for generating conditional knockout mutations. Genome Res 13: 476-484, 2003.
21. Sarov M, Schneider S, Pozniakovski A, Roguev A, Ernst S, Zhang Y, Hyman AA and Stewart AF: A recombineering pipeline for functional genomics applied to *Caenorhabditis elegans*. Nat Methods 3: 839-844, 2006.
22. Rohrschneider LR, Rothwell VM and Nicola NA: Transformation of murine fibroblasts by a retrovirus encoding the murine c-fms proto-oncogene. Oncogene 4: 1015-1022, 1989.
23. Lacey DL, Timms E, Tan HL, Kelley MJ, Dunstan CR, Burgess T, Elliott R, Colombero A, Elliott G, Scully S, *et al*: Osteoprotegerin ligand is a cytokine that regulates osteoclast differentiation and activation. Cell 93: 165-176, 1998.
24. Yao GQ, Wu JJ, Troiano N, Zhu ML, Xiao XY and Insogna K: Selective deletion of the membrane-bound colony stimulating factor 1 isoform leads to high bone mass but does not protect against estrogen-deficiency bone loss. J Bone Miner Metab 30: 408-418, 2012.
25. Kawano T, Zhu M, Troiano N, Horowitz M, Bian J, Gundberg C, Kolodziejczak K and Insogna K: LIM kinase 1 deficient mice have reduced bone mass. Bone 52: 70-82, 2013.
26. Perona R, Montaner S, Saniger L, Sánchez-Pérez I, Bravo R and Lacal JC: Activation of the nuclear factor-kappaB by Rho, CDC42, and Rac-1 proteins. Genes Dev 11: 463-475, 1997.
27. Montaner S, Perona R, Saniger L and Lacal JC: Multiple signalling pathways lead to the activation of the nuclear factor kappaB by the Rho family of GTPases. J Biol Chem 273: 12779-12785, 1998.
28. Miyazaki T, Katagiri H, Kanegae Y, Takayanagi H, Sawada Y, Yamamoto A, Pando MP, Asano T, Verma IM, Oda H, *et al*: Reciprocal role of ERK and NF-kappaB pathways in survival and activation of osteoclasts. J Cell Biol 148: 333-342, 2000.
29. Ogasawara T1, Katagiri M, Yamamoto A, Hoshi K, Takato T, Nakamura K, Tanaka S, Okayama H and Kawaguchi H: Osteoclast differentiation by RANKL requires NF-kappaB-mediated down-regulation of cyclin-dependent kinase 6 (Cdk6). J Bone Miner Res 19: 1128-1136, 2004.
30. Yao C, Yao GQ, Sun BH, Zhang C, Tommasini SM and Insogna K: The transcription factor T-box3 regulates colony stimulating factor 1-dependent Jun dimerization protein 2 expression and plays an important role in osteoclastogenesis. J Biol Chem 289: 6775-6790, 2014.
31. Lloyd SA, Yuan YY, Kostenuik PJ, Ominsky MS, Lau AG, Morony S, Stolina M, Asuncion FJ and Bateman TA: Soluble RANKL induces high bone turnover and decreases bone volume, density, and strength in mice. Calcif Tissue Int 82: 361-372, 2008.
32. Frost JA, Swantek JL, Stippec S, Yin MJ, Gaynor R and Cobb MH: Stimulation of NFkappa B activity by multiple signaling pathways requires PAK1. J Biol Chem 275: 19693-19699, 2000.
33. Boyer L, Travaglione S, Falzano L, Gauthier NC, Popoff MR, Lemichez E, Fiorentini C and Fabbri A: Rac GTPase instructs nuclear factor-kappaB activation by conveying the SCF complex and IkBalpha to the ruffling membranes. Mol Biol Cell 15: 1124-1133, 2004.
34. Michaelson D, Abidi W, Guardavaccaro D, Zhou M, Ahearn I, Pagano M and Philips MR: Rac1 accumulates in the nucleus during the G2 phase of the cell cycle and promotes cell division. J Cell Biol 181: 485-496, 2008.
35. van Hennik PB, ten Klooster JP, Halstead JR, Voermans C, Anthony EC, Divecha N and Hordijk PL: The C-terminal domain of Rac1 contains two motifs that control targeting and signaling specificity. J Biol Chem 278: 39166-39175, 2003.
36. Sandrock K, Bielek H, Schradi K, Schmidt G and Klugbauer N: The nuclear import of the small GTPase Rac1 is mediated by the direct interaction with karyopherin alpha2. Traffic 11: 198-209, 2010.
37. Vaira S, Alhawagri M, Anwisye I, Kitaura H, Faccio R and Novack DV: RelA/p65 promotes osteoclast differentiation by blocking a RANKL-induced apoptotic JNK pathway in mice. J Clin Invest 118: 2088-2097, 2008.
38. Ikeda F, Matsubara T, Tsurukai T, Hata K, Nishimura R and Yoneda T: JNK/c-Jun signaling mediates an anti-apoptotic effect of RANKL in osteoclasts. J Bone Miner Res 23: 907-914, 2008.